

Resolution-dependent quark masses from meson correlators

Hilmar Forkel^{a,b} and Kai Schwenzer^a

(a) *Institut für Theoretische Physik, Universität Heidelberg, D-69120 Heidelberg, Germany*

(b) *Institut für Theoretische Physik II, Ruhr-Universität Bochum, D-44780 Bochum, Germany*

We explore the impact of a resolution-dependent constituent quark mass, as recently applied to diffractive meson production, in QCD correlation functions of several spin-0 and spin-1 meson channels. We compare the resulting correlators with experimental and lattice data, analyze the virtues and limitations of the approach, and discuss the channel dependence of the obtained effective quark masses.

I. INTRODUCTION

The constituent quarks of the “naive”, nonrelativistic quark model are universal, i.e. hadron-channel independent degrees of freedom with a flavor-dependent but otherwise constant mass. This simple concept has been refined in several relativistic quark models. Usually, then, the quarks become “dressed” quasi-particles and their constituent mass turns into a momentum-dependent mean field or self-energy.

Constituent-quark masses with a different kind of momentum dependence have recently been employed for the description of diffractive vector-meson production processes in Ref. [1]. Guided by analogy with a nonrelativistic quark-model amplitude, the authors of [1] model the vector polarization function in terms of a resolution-dependent quark mass (RDQM) $m_{\text{eff}}(Q^2)$, similar to the cutoff-dependent quark masses generated during renormalization group (RG) evolution [2] of chiral quark models [3, 4]. Since this approach has proven quite successful in reproducing experimental data for the vector polarization amplitude, it seems worthwhile to explore its uses in a broader setting, i.e. in correlation functions of other important meson channels. This is the aim of the present note.

The specific implementation of the resolution-dependent quark mass in Ref. [1], namely as a replacement of the constant quark mass in the otherwise noninteracting correlators, lets one suspect that not the whole variety of physics in other meson channels can be captured in such a minimal way. In this regard the spin-0 correlators hold a particular challenge since their behavior can be qualitatively altered by the underlying vacuum physics. The strength of the interaction in the pseudoscalar isovector correlator, for example, gets up to two orders of magnitude larger than in the vector channel, and it sets in at smaller distances [5, 6]. Of course, this behavior is naturally explained by the spontaneous breakdown of chiral symmetry in the QCD vacuum and reflects the exceptionally strong attraction needed to generate almost massless Goldstone pions.

The pronounced differences in the behavior of the various mesonic correlators raise the question to which extent they can be described by a *universal* resolution (and flavor) dependent mass with an at least approximately channel-independent momentum dependence. Such a channel independence appears natural from the perspective of the naive quark model. Indeed, the spectroscopic successes of the latter suggest that important bulk features of most hadrons can be understood on the basis of universal constituent-quark properties, and especially without assuming their internal structure, as revealed by their momentum dependence, to depend on the hadron state considered.

Our strategy for exploring the virtues and limitations of the RDQM method beyond the vector channel will rely mainly on a comparison of the resulting meson correlators with those obtained from other, as far as possible model-independent sources. As such input sources we employ experimental data, phenomenological estimates, and lattice results on point-to-point correlators. The latter constitute our main input in the spin-0 channels, which are not directly accessible to experimental probes. After outlining our calculational setup, we discuss generic properties of the resulting RDQMs and then proceed to their quantitative analysis. Finally, we present our conclusions and offer a few speculations about improved implementations of resolution-dependent masses.

II. MESONIC CORRELATORS WITH RESOLUTION-DEPENDENT QUARK MASSES

QCD correlation functions of interpolating currents with hadronic quantum numbers link hadron properties rather directly to quark properties. Hence they provide a suitable framework for phenomenological studies of resolution-dependent quark masses. The first such investigation [1] dealt with the correlator of two vector currents at spacelike momentum transfer and modeled several diffractive high-energy processes on its basis. Despite some motivation for this approach by an harmonic oscillator quark-model analogy for the photon wave function [1], however, the physical foundations and the implementation of the method deserve further study.

As a step in this direction, we will generalize the RDQM approach below to the light meson correlators

$$\Pi^{(i)}(x) = \langle 0 | T J^{(i)}(x) J^{(i)\dagger}(0) | 0 \rangle \quad (1)$$

in those Lorentz channels for which phenomenological and lattice data exist. Hence we consider the isovector currents $J^{(i)} = \bar{u}\Gamma^{(i)}d$ in the channels i specified by $\Gamma^{(i)} \in \{1, i\gamma_5, \gamma^\mu, \gamma^\mu\gamma_5\}$. The Fourier transform of $\Pi^{(i)}(x)$ yields the polarization tensors

$$\tilde{\Pi}^{(i)}(q) = \int d^4z e^{iq \cdot x} \Pi^{(i)}(x) \equiv \Pi^{(i)}(q^2) K^{(i)}(q) \quad (2)$$

which we have factorized into an invariant amplitude $\Pi^{(i)}(q^2)$ and a Lorentz tensor $K^{(i)}(q)$ with

$$K^{(s)}(q) = K^{(p)}(q) = 1, \quad (3)$$

$$K^{(v)}(q) = K^{(at)}(q) = q^\mu q^\nu - q^2 g^{\mu\nu}, \quad (4)$$

$$K^{(al)}(q) = q^\mu q^\nu. \quad (5)$$

Here the superscripts denote the scalar (s), pseudoscalar (p), vector (v), as well as the longitudinal (al) and transverse (at) components of the axial-vector channel. The invariant amplitudes have the usual spectral representation

$$\Pi^{(i)}(Q^2 = -q^2) = \frac{1}{\pi} \int_0^\infty ds \frac{\text{Im}\Pi^{(i)}(s)}{s + Q^2}. \quad (6)$$

We do not write subtraction terms explicitly since they will not enter our determination of the resolution-dependent masses.

A. Resolution-dependent quark masses

In this section we establish the basic formalism for obtaining resolution-dependent constituent masses $m_{\text{eff}}(\nu^2)$ from data on the meson correlators. To this end, we generalize the procedure of Ref. [1] where a model for the second Q^2 -derivative of the physical vector correlator $\Pi^{(v)}(Q^2)$ was obtained by supplying the free quarks in the noninteracting vector correlator $\Pi_0^{(v)}$ with a resolution-dependent mass and by identifying the resolution scale ν with the momentum transfer Q . The derivatives with respect to Q^2 were taken mainly in order to remove the UV singularity of $\Pi_0^{(v)}$. A straightforward generalization of this procedure yields our model for the mesonic correlator amplitudes and their n -th derivative in the channel i ,

$$\Pi_{\text{mod},n}^{(i)}(Q^2, m_{\text{eff}}) = \left. \frac{\partial^n}{\partial (-Q^2)^n} \Pi_0^{(i)}(Q^2, m_0) \right|_{m_0 \rightarrow m_{\text{eff}}(Q^2)}, \quad (7)$$

where $\Pi_0^{(i)}$ are the invariant amplitudes of the free correlators

$$\tilde{\Pi}_0^{(i)}(-q^2, m_0) = iN_c \int \frac{d^4k}{(2\pi)^4} \text{tr}[S(k)\Gamma^{(i)}S(k+q)\Gamma^{(i)}] \quad (8)$$

and $S(k) = (\not{k} - m_0 + i\epsilon)^{-1}$ denotes the noninteracting fermion propagator.

In dimensional regularization, the free correlator amplitudes at spacelike momenta $Q^2 \equiv -q^2 > 0$ read

$$\Pi_0^{(s)}(Q^2) = \frac{N_c}{8\pi^2} Q^2 \left\{ (1+\rho)^{\frac{3}{2}} \log\left(\frac{\sqrt{1+\rho}+1}{\sqrt{1+\rho}-1}\right) - 2\rho - \frac{5}{3} - \left(1 + \frac{3\rho}{2}\right) \left[\frac{2}{\epsilon} - \gamma + \log(4\pi) + \log\left(\frac{\mu^2}{m_0^2}\right)\right] \right\} \quad (9)$$

$$\Pi_0^{(p)}(Q^2) = \frac{N_c}{8\pi^2} Q^2 \left\{ \sqrt{1+\rho} \log\left(\frac{\sqrt{1+\rho}+1}{\sqrt{1+\rho}-1}\right) - \frac{5}{3} - \left(1 + \frac{\rho}{2}\right) \left[\frac{2}{\epsilon} - \gamma + \log(4\pi) + \log\left(\frac{\mu^2}{m_0^2}\right)\right] \right\} \quad (10)$$

for the spin-0 channels and

$$\Pi_0^{(v)}(Q^2) = -\frac{N_c}{12\pi^2} \left\{ \left(1 - \frac{\rho}{2}\right) \sqrt{1+\rho} \log\left(\frac{\sqrt{1+\rho}+1}{\sqrt{1+\rho}-1}\right) + \rho - \frac{5}{3} - \left[\frac{2}{\epsilon} - \gamma + \log(4\pi) + \log\left(\frac{\mu^2}{m_0^2}\right)\right] \right\} \quad (11)$$

$$\Pi_0^{(at)}(Q^2) = -\frac{N_c}{12\pi^2} \left\{ (1+\rho)^{\frac{3}{2}} \log\left(\frac{\sqrt{1+\rho}+1}{\sqrt{1+\rho}-1}\right) - 2\rho - \frac{5}{3} - \left(1 + \frac{3\rho}{2}\right) \left[\frac{2}{\epsilon} - \gamma + \log(4\pi) + \log\left(\frac{\mu^2}{m_0^2}\right)\right] \right\} \quad (12)$$

$$\Pi_0^{(al)}(Q^2) = \frac{N_c}{8\pi^2} \rho \left\{ \sqrt{1+\rho} \log\left(\frac{\sqrt{1+\rho}+1}{\sqrt{1+\rho}-1}\right) - 2 - \left[\frac{2}{\epsilon} - \gamma + \log(4\pi) + \log\left(\frac{\mu^2}{m_0^2}\right)\right] \right\} \quad (13)$$

for the spin-1 channels. Above, we have introduced the abbreviation $\rho \equiv 4m_0^2/Q^2$, the regulator $\epsilon \equiv 4-d$, and its mass scale μ . As anticipated, the divergent pieces (corresponding to subtraction terms in the dispersive representation) can be made to vanish by taking a sufficient number of derivatives with respect to Q^2 . This will always be ensured below. Hence the above expressions, together with the prescription (7) for the $\Pi_{\text{mod},n}^{(i)}(Q^2, m_{\text{eff}})$, uniquely define our model for the interacting meson correlators.

At this point, it might be useful to emphasize a crucial difference between the resolution-dependent quark masses $m(\nu^2)$ defined above and the more conventional momentum-dependent self-energies which are encountered, e.g., in quark or instanton-vacuum models. In contrast to the latter, the RDQM does *not* depend on the loop momentum k flowing through the quark propagators, but rather on the overall momentum transfer Q which is assumed to set the resolution scale ν of the constituent quarks. This is analogous to the usual renormalization-group improvement of perturbation theory, where the running RG scale of coupling and mass parameters is similarly identified with the external momentum scale [17].

The identification of the scale ν with the overall momentum Q , i.e. with a variable not associated with the individual quarks but rather with the (channel-dependent) correlator as a whole, raises the crucial issue of channel dependence for the resolution-dependent quark mass.

B. Representation of input data and matching procedure

Information from several independent sources, including dispersive fits to experimental data in the spin-1 channels, QCD sum rules and lattice simulations of point-to-point correlators, indicate that the detailed structure of the spectral functions $\text{Im}\Pi^{(i)}/\pi$ is strongly channel-dependent [6]. Nevertheless, most channels have two qualitative features in common: (i) only the lowest resonance in a given channel is clearly separated and fully resolved whereas the higher-lying ones increasingly merge with the multi-particle continuum, and (ii) local duality [7] implies that the hadronic continuum, when averaged over suitable invariant-mass intervals, can be approximated by the free-quark continuum in the same channel.

Hence the available experimental and lattice data on the considered meson correlators are (within their partially substantial errors, see below) well described by a parametrization of the spectral functions in terms of a zero-width ground state pole and an effective continuum:

$$\text{Im}\Pi_{\text{data}}^{(i)}(s) = \pi\lambda_i^2\delta(s - m_i^2) + \text{Im}\Pi_0^{(i)}(s)\theta(s - s_{0,i}). \quad (14)$$

This efficient and transparent parametrization, originally designed for QCD sum rules [8], has by now become fairly standard in hadron correlator phenomenology [6]. It depends on only three parameters: the mass m_i and coupling λ_i of the lowest resonance in the meson channel i and the corresponding threshold $s_{0,i}$. Note that local duality implies $s_{0,i} > m_i^2$. The required spectral functions $\text{Im}\Pi_0^{(i)}$ for noninteracting quarks are obtained by analytically continuing

Eqs. (9) - (13):

$$\text{Im}\Pi_0^{(s)}(s) = \frac{N_c}{8\pi} \theta(s - 4m_0^2) s \sqrt{\left(\frac{s - 4m_0^2}{s}\right)^3}, \quad (15)$$

$$\text{Im}\Pi_0^{(p)}(s) = \frac{N_c}{8\pi} \theta(s - 4m_0^2) s \sqrt{\frac{s - 4m_0^2}{s}}, \quad (16)$$

$$\text{Im}\Pi_0^{(v)}(s) = \frac{N_c}{12\pi} \theta(s - 4m_0^2) \frac{s + 2m_0^2}{s} \sqrt{\frac{s - 4m_0^2}{s}}, \quad (17)$$

$$\text{Im}\Pi_0^{(at)}(s) = \frac{N_c}{12\pi} \theta(s - 4m_0^2) \sqrt{\left(\frac{s - 4m_0^2}{s}\right)^3}, \quad (18)$$

$$\text{Im}\Pi_0^{(al)}(s) = \frac{N_c}{8\pi} \theta(s - 4m_0^2) \frac{4m_0^2}{s} \sqrt{\frac{s - 4m_0^2}{s}}. \quad (19)$$

Although local duality approximately relates the effective thresholds $s_{0,i}$ to properties of the ground-state resonances via finite-energy sum rules, we prefer to keep them independent in order to achieve a less biased representation of the input data.

We can now determine $m_{\text{eff}}^{(i)}(Q^2)$ - independently in each channel i - by equating Q^2 -derivatives of our model correlator amplitudes, given by Eq. (7), to different sets of input data in the above parametrization. Specifically, we will match the second derivatives $\Pi^{(2)}$ since $n = 2$ is the minimal number which renders all free correlators UV-finite and since higher derivatives tend to increasingly impair the numerical analysis [18]. We will refer to this procedure as the (minimal) ‘‘RDQM approach’’. To summarize the above discussion, our resolution-dependent quark masses $m_{\text{eff}}^{(i)}(Q^2)$ are solutions of the equation

$$\left. \frac{\partial^2 \Pi_0^{(i)}(Q^2, m_0)}{\partial (Q^2)^2} \right|_{m_0 \rightarrow m_{\text{eff}}^{(i)}(Q^2)} = \frac{2\lambda_i^2}{(m_i^2 + Q^2)^3} + \frac{2}{\pi} \int_{s_{0,i}}^{\infty} ds \frac{\text{Im}\Pi_0^{(i)}(s, m_0)}{(s + Q^2)^3} \quad (20)$$

in the channel i . In channels where $m_{\text{eff}}^{(i)}$ reaches zero at a finite Q_c^2 it is assumed to remain zero for all $Q^2 > Q_c^2$ (or, more precisely, for Q^2 larger than the smallest Q_c^2 if there should be more than one, see below).

It remains to fix the three hadronic input parameters on the right-hand side of Eq. (20). In the analysis of the vector correlator in Ref. [1] the physical values of m_v and λ_v where used, while $s_{0,v}$ was obtained from a finite-energy sum rule [19]. Since direct experimental data on the momentum dependence of the meson correlators are available in the vector channel only, we have to resort to other sources for determining the parameters m_i , λ_i and $s_{0,i}$ in the other channels. Those will include the phenomenological estimates by Shuryak [6] and two sets of lattice data on point-to-point correlators [9, 10] (both extrapolated to the chiral and continuum limits) which are, at least in principle, free of uncontrolled model assumptions [20]. The statistical and likely also the systematic errors of the lattice data [21] are still uncomfortably large, however.

The numerical values of m_i , λ_i and $s_{0,i}$ resulting from the different data sets are listed in the left part of Table I. For later use, we note that the correlators calculated in the instanton liquid model (ILM) [14] are also well represented in the pole-duality parametrization, and their predictions for the meson parameters have been included in Table I for comparison. The spacetime correlators corresponding to our input data sets in the respective channels, normalized to the free correlators, are plotted in Fig. 1. Most data are available for the vector correlator which has been measured in e^+e^- annihilation experiments and is, at low momenta, dominated by the ρ -meson. The lowest resonance in the transverse axial-vector channel is the heavier a_1 meson. In both channels we use Shuryak’s phenomenological analysis of the experimental data [6] and the masses given by the Particle Data Group [15]. The scalar isovector channel is singled out by the absence of an established ground-state resonance. The pseudoscalar channel, on the other hand, is strongly dominated by the pion resonance with its exceptionally small mass and large coupling. For this reason, its ratio with the corresponding free correlator exceeds those in the other meson channels by up to two orders of magnitude.

III. QUALITATIVE BEHAVIOR OF THE SCALE-DEPENDENT QUARK MASS

Before embarking on the numerical solution of Eq. (20) it will be useful to establish several qualitative properties of the resulting resolution-dependent masses and their channel dependence. Besides providing useful checks and constraints for our subsequent numerical analysis, they will shed light on generic features of the RDQM approach.

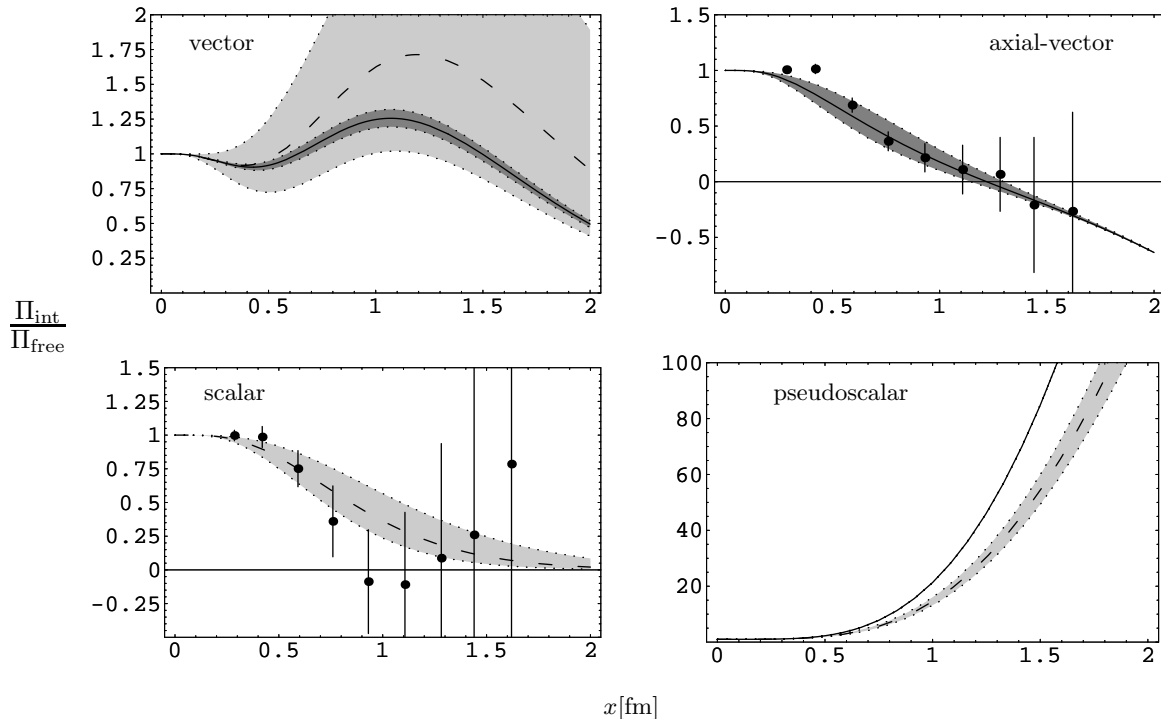


FIG. 1: The resonance continuum parametrization of the ratio $\Pi_{\text{int}}/\Pi_{\text{free}}$ of interacting and free coordinate space correlators in the channels considered. Solid lines with dark error bands represent the phenomenological correlators [6], whereas dashed lines with brighter (statistical) error bands represent the lattice correlators [9]. In the scalar channel the curve shows our fit to the lattice data (dots), whereas no significant fit to the shown lattice data was possible in axial-vector channel. Note that in the vector channel the error of the given fit is much larger than the error of the original lattice data [9].

A. Constituent quark masses

To start with, let us consider the $Q^2 \rightarrow 0$ limit of Eq. (20), which has the analytic solutions

$$m_{\text{eff}}^{(s)}(0) = \frac{\sqrt{s_0}}{\sqrt{10}}, \quad m_{\text{eff}}^{(p)}(0) = \frac{\sqrt{s_0}}{\sqrt{6(1 + \frac{8}{3}\pi^2\alpha_p^2)}}, \quad (21)$$

$$m_{\text{eff}}^{(v)}(0) = \frac{\sqrt{s_0}}{\sqrt[4]{\frac{70}{3}(1 + 8\pi^2\beta_v^2)}}, \quad m_{\text{eff}}^{(at)}(0) = \frac{\sqrt{s_0}}{\sqrt[4]{70(1 + 8\pi^2\beta_{at}^2)}}. \quad (22)$$

The resonance parameters enter these expressions in the combinations

$$\alpha_i \equiv \frac{\sqrt{s_{0,i}}\lambda_i}{m_i^3} \quad (\text{spin-0}), \quad \beta_i \equiv \frac{s_{0,i}\lambda_i}{m_i^3} \quad (\text{spin-1}). \quad (23)$$

The numerical values of the $m_{\text{eff}}^{(i)}(0)$, as obtained from the various input parameter sets, are listed in the fifth column of Table I. With $\sqrt{10} \approx 3.2$ and typical continuum threshold scales $s_{0,i} \approx 1$ GeV one obtains masses of the order $m_{\text{eff}}(0) \sim 200 - 350$ MeV - i.e. in the range expected for constituent quarks - in all but the pseudoscalar channel. This holds even in the scalar channel where no resonance is resolved (i.e. $\lambda_s = 0$) in any of the input data sets.

The qualitative behavior of the $m_{\text{eff}}^{(i)}(0)$ can be understood by noting that the input values for couplings and continuum thresholds are of comparable size in all channels. Therefore, the resonance masses generate the main distinction between the channels. This is particularly obvious in the pseudoscalar channel where the mass of the resonance is exceptionally small. As a consequence, α_p dominates the denominator of (21) and the pseudoscalar constituent quark becomes unrealistically light, of the order of the light current masses: $m_{\text{eff}}^{(p)}(0) \propto m_p^2$. We have thus

found first evidence for a strong channel dependence of our RDQM procedure. It does not really come as a surprise, though, because the (quasi-) Goldstone pion cannot be consistently described in the constituent quark model, from which the RDQM approach draws part of its motivation. An artificially small constituent mass is also obtained from the longitudinal part of the axial-vector correlator since partial conservation of the axial-vector current (PCAC) [16] relates it to the pseudoscalar correlator as

$$\Pi^{(al)}(Q^2) = \frac{4m_0^2}{Q^4} \Pi^{(p)}(Q^2). \quad (24)$$

We have therefore not given the corresponding mass formula separately.

B. Chiral restoration

A characteristic property of resolution-dependent effective quark masses, expected on physical grounds and confirmed in Ref. [1], is that they decrease with growing resolution Q^2 . Moreover, the mass of Ref. [1] was found to vanish (for $m_0 = 0$) at a critical scale $Q_c \sim 1$ GeV, in accord with the expectation that the massive “cloud” of a constituent quark disappears when probed hard enough to resolve the massless current quark. The vanishing of m_{eff} has been interpreted as a signature of chiral restoration since constituent quarks owe their mass to spontaneous chiral symmetry breaking and since the “critical momentum” $Q_c \sim 1$ GeV is compatible with the scale $\Lambda_\chi \simeq 4\pi f_\pi \sim 1.2$ GeV around which one expects chiral symmetry to be restored. In the spin-1 channels chiral symmetry even becomes manifest since the noninteracting spin-1 correlators are chirally invariant in the zero-quark-mass limit.

Since chiral symmetry and its spontaneous breaking are determining features of hadron physics one would expect the restoration transition towards $m_{\text{eff}}^{(i)}(Q_c^2) = 0$ to be a generic and robust property of resolution-dependent constituent masses. In particular, one would hope that the RDQM approach outlined above yields such a behavior in all correlator channels. Below we will establish the conditions under which this is possible. More specifically, we will obtain necessary and sufficient criteria for the existence and number of solutions of Eq. (20) at zero quark mass. To this end, we rewrite Eq. (20) in the chiral limit by isolating the pole piece on the right-hand side (and multiplying by $\pi/2$). This yields

$$\int_0^{s_0} ds \frac{\text{Im}\Pi_0^{(s/p)}(s, m=0)}{(s+Q_c^2)^3} = \frac{N_c}{16\pi} \frac{s_0^2}{Q_c^2 (s_0+Q_c^2)^2} = \frac{\pi\lambda_{s/p}^2}{(m_{s/p}^2 + Q_c^2)^3} \quad (25)$$

for the spin-0 channels and

$$\int_0^{s_0} ds \frac{\text{Im}\Pi_0^{(v/at)}(s, m=0)}{(s+Q_c^2)^3} = \frac{N_c}{24\pi} \frac{s_0 (s_0 + 2Q_c^2)}{Q_c^4 (s_0 + Q_c^2)^2} = \frac{\pi\lambda_{v/at}^2}{(m_{v/at}^2 + Q_c^2)^3} \quad (26)$$

for the spin-1 channels [22]. If solutions Q_c to these equations exist, the lowest one of them determines the transition point at which the RDQMs vanish. Due to the chiral symmetry of noninteracting, massless quarks the left-hand sides of the above equations are identical for both parities in the spin-0 as well as spin-1 channels.

Although the solutions of Eqs. (25) and (26) can be obtained analytically, they do not lend themselves easily to a transparent discussion. We therefore extract the required information on existence and number of solutions directly from the equations. Relegating details of the corresponding analysis to the appendix, we just list the main results here. The most general finding is that, independent of the channel, both equations (25) and (26) can have either zero, one or two solutions Q_c^2 , depending on the values of the 3 hadronic parameters m^2 , λ^2 and s_0 . If two solutions Q_c^2 exist, then by continuity the smaller is the physical one. In the absence of a pole (i.e. for $\lambda_i^2 = 0$), furthermore, the only positive solution is $Q_c^2 = \infty$. In all other cases, Q_c^2 decreases with increasing resonance strength λ_i^2 and with decreasing pole mass m_i . This implies, in particular, that Q_c^2 will be smallest in the pion channel. Several additional properties of the solutions depend on the spin of the underlying correlator:

1. In the spin-0 channels, the further analysis of Eq. (25) requires to distinguish the two domains $s_0 \leq 3m_{s/p}^2/2$. For $s_0 > 3m_{s/p}^2/2$, which holds naturally in the Goldstone boson channel, and for $s_0^2 < 16\pi^2\lambda_{s/p}^2/N_c$, which is additionally satisfied by the pseudoscalar input parameter sets in Table I, we predict a single solution and find an upper bound on Q_c [23] given by

$$Q_c^2 \leq \frac{s_0 m_{s/p}^2}{2s_0 - 3m_{s/p}^2}. \quad (27)$$

(Note that this bound does not apply to our data sets in the scalar channel since m_s^2 cannot be resolved in this case, see below.) Moreover, we note that for the typical $s_{0,p} \sim 1$ GeV and $m_p \sim 0.14$ GeV found in Table I, the bound (27) becomes unrealistically small, $Q_c < 0.1$ GeV. In the scalar channel, on the other hand, no pole term can be extracted from the data, i.e. $\lambda_s^2 = 0$. Inspection of Eq. (25) immediately shows that the scale-dependent quark mass cannot vanish at any finite resolution in this case. This entails another channel-dependence of the RDQM procedure (if it is not simply a shortcoming of our input data in the scalar channel).

2. In the spin-1 channels, we have again to distinguish between two domains of s_0 -values: for $m_{v/at}^2 < s_0 < 2m_{v/at}^2$, which is satisfied by part of our input data in the vector channel and all of them in the axial-vector channel, we find a finite solution for $24\pi^2\lambda_{v/at}^2/N_c > 2s_0$ and none otherwise. For $s_0 > 2m_{v/at}^2$, which is satisfied by the remaining part of our input data in the vector channel, Eq. (26) can again have either one or no physical solution, depending on which parameter set in Table I is considered. For $s_0 > 2m_{v/at}^2$ there is an upper bound on Q_c^2 , given by

$$Q_c^2 \leq \frac{s_0}{6(2m_{v/at}^2 - s_0)} \left[s_0 - 6m_{v/at}^2 - \sqrt{(s_0 + 6m_{v/at}^2)^2 - 48m_{v/at}^4} \right], \quad (28)$$

which can be somewhat sharpened in case of a unique solution (see appendix).

Given an input data set for a correlator with the corresponding values for m , λ and s_0 , the above results instantly reveal whether the extracted m_{eff} will vanish at some finite Q_c . With the data in Table I we predict a vanishing effective quark mass in the pseudoscalar channel as well as in the vector channel for the phenomenological, lattice I and II, but not for the ILM data, and no ‘‘chiral restoration’’ in the axial-vector channel (the ILM data in this channel are excluded from this consideration since they do not satisfy $m_{at}^2 < s_0$). These predictions hold for the central values of the input parameter sets and are confirmed by our numerical analysis below. Inside the rather large error range of the input parameter space in the vector channel there are also regions, however, in which no solution for Q_c^2 exists.

Moreover, our above findings show that both the existence and the scale of the ‘‘critical momentum’’ Q_c are rather sensitive to the values of the hadronic input parameters. For $Q_c \gg \Lambda_\chi \sim 1$ GeV, this dependence becomes so strong that details of the input data inside their systematic and statistical error range would contaminate the results. However, critical momenta of such a magnitude well beyond typical hadronic and restoration scales would have to be excluded anyhow on physical grounds, and their occurrence is strongly restricted (for reasonable values of the hadronic parameters) by the bounds (27) and (28). Finally, the above analysis shows that the RDQM procedure yields a well-defined and, in conjunction with the monotonicity of the $m_{\text{eff}}(Q^2)$, a unique Q^2 -dependence of the resolution-dependent quark masses once the input parameters are fixed.

C. Generic limitations

A few additional limitations of the RDQM approach can be understood without numerical analysis. First and probably foremost, one should not expect this method to reproduce the exceptional properties of the pseudoscalar correlator, despite our observation that spontaneous chiral symmetry breaking and restoration are to some extent incorporated. We have found above, for example, that the pion pole contribution can only be matched with almost vanishing, i.e. unacceptably small constituent quark masses (cf. Table I). This is consistent with the fact that the RDQM approach derives its main motivation [1] from an analogy with the nonrelativistic quark model. Indeed, the latter also fails to describe the pion because it cannot provide the strong binding required by Goldstone’s theorem. More generally, one might expect the RDQM approach to be overburdened in channels which contain exceptionally strongly bound states and to be more useful in channels where the lowest-lying resonances are quark-model states (including, e.g., the heavy-quark sector).

Another qualitative limitation of the RDQM approach is related to the channel-dependence of broken internal symmetries. Within the set of channels which we consider in this paper, this is most explicitly demonstrated for isospin symmetry. The underlying assumption of an isospin-symmetric effective mass, together with the isospin invariance of the free correlators, implies that the RDQM approach yields the same correlators in the scalar-isoscalar and scalar-isovector channels [24]. The physical correlators in those two channels, however, differ rather strongly [25]. In fact, lattice and instanton-liquid simulations as well as phenomenological estimates even find them to have opposite signs, indicating a rather strong attraction in the isoscalar and a similarly strong repulsion in the isovector channel [14]. This and other substantial differences cannot be captured by resolution-dependent quark masses *alone*. Even the introduction of an unrealistically large up/down constituent mass difference, at the price of a strong departure from universality and good isospin, would not be able to reproduce, e.g., the sign difference.

IV. QUANTITATIVE ANALYSIS

In the following section, we discuss the results of determining the resolution-dependent quark masses according to the procedure described in section II B, i.e. by solving Eq. (20) numerically for $m_{\text{eff}}^{(i)}(Q^2)$ in the channels i under consideration. Of course, the exact solutions of Eq. (20) do constitute neither the most reliable nor the most exhaustive use of the information contained in the input data. In view of the considerable (both statistical and systematic) errors of the latter, an only approximate matching between data and model correlators inside some error margins should result in a better representation of the physics which they contain. Since the implementation of such a procedure would introduce additional ambiguity, however, we will instead just propagate the error ranges of the input data sets in order to get a measure for the errors of the resulting $m_{\text{eff}}^{(i)}(Q^2)$.

		m [MeV]	λ [MeV]	$\sqrt{s_0}$ [MeV]	$m_{\text{eff}}(Q^2=0)$ [MeV]	Q_c^2 [MeV ²]
vector	phenomenology	780	214±6	1590±20	227±15	1320-318+528
	lattice I	720±60	233±47	1620±230	193±44	464-259+1957
	lattice II	690±170	209±163	1400±400	191±159	531-475+∞
	ILM	950±100	160±38	1500±100	347±92	-
axial-vector (transverse)	phenomenology	1230±40	152±22	1600±100	381±42	-
	ILM	1132±50	82±15	1100±50	351±27	-
		m [MeV]	$\sqrt{\lambda}$ [MeV]	$\sqrt{s_0}$ [MeV]	$m_{\text{eff}}(Q^2=0)$ [MeV]	Q_c^2 [MeV ²]
scalar	lattice I	-	-	955±213	338±40	-
pseudoscalar	phenomenology	138	480	≈ 1600	0.9±0.1	2.5±0.1
	lattice I	156±10	440±10	< 1000	1.6±0.1	7.3±1.0
	ILM	142±14	510±20	1360±100	0.9±0.1	2.3±2.5

TABLE I: The parameters of the resonance continuum fit to the input meson correlators of Refs. [6], [15] (phenomenological analysis of e^+e^- annihilation and τ -decay data), [9] (lattice simulation I by Chu et al.), [10] (lattice simulation II by Hands et. al.), and finally [14] (random instanton liquid model (ILM)). The phenomenological continuum threshold in the axial vector channel was estimated in [6]. The table also contains our results for the constituent masses and the critical momenta (where they exist). (The infinite upper bound on $Q_{c,v}^2$ from the lattice II data in the vector channel corresponds to the particular parameter combination $s_0 = 2m_v^2$ (cf. Eq. (28)) which lies inside the error range of the input data.)

The results of our quantitative analysis are collected in Table I and in Figs. 2-4. Besides the values of the critical momenta Q_c^2 (for the parameter sets where they exist) with their error bands, the numerical values of the quark masses at zero momentum transfer are listed in the right part of Table I. As already mentioned, one finds typical constituent quark masses of the order $250 \text{ MeV} \lesssim m_{\text{eff}} \lesssim 350 \text{ MeV}$ in all channels except the pseudoscalar one. The more detailed properties of the resulting $m_{\text{eff}}^{(i)}(Q^2)$ turn out to be channel-specific:

1. In the pseudoscalar channel we encounter unrealistically small scales for $m_{\text{eff}}^{(p)}$ and Q_c^2 , owing to the underrepresentation of Goldstone-mode physics. Even if one would insist on fitting the pseudoscalar correlators by tolerating the necessarily too small $m_{\text{eff}}^{(p)}$, however, the matching would still fail for all $Q^2 > Q_c^2 \sim 5 \text{ MeV}^2$ since the free, massless correlator cannot reproduce the strong rise found in the input data (cf. Fig. 1). This shortcoming acquires additional significance in view of the fact that this rise, and pionic physics in general, is probably underrepresented in the quenched lattice data of [9] and [10] (which yield rather large pion masses). As mentioned above, the relation between pseudoscalar and longitudinal axial-vector correlators (cf. Eq. (24)) implies that the latter is beyond the reach of the RDQM approach, too, and does not require independent discussion.
2. In the vector channel, the extracted, resolution-dependent quark masses interpolate monotonically between reasonable constituent mass values at $Q = 0$ and zero [26] at the “critical” scale Q_c . This general behavior is in accord with the findings of Ref. [1] which were obtained in the same channel. The resulting Q -dependence of $m_{\text{eff}}(Q^2)$ is closest to the scale dependence of constituent masses which one would expect on the basis of the qualitative arguments given above. It is plotted in Fig. 2. As a consequence of our different input data sets and their rather large errors, however, we find a similarly large range of values for Q_c . This is a further indication for the mostly qualitative character of the estimates for m_{eff} which can be obtained from the RDQM approach.

3. The transverse axial-vector channel shares several common features with the vector channel. In particular, both noninteracting amplitudes become equal for zero quark mass. The main difference, at least in the duality-based continuum parametrization of the input data, is the about 60% larger resonance mass. It results in a much smaller (negative) slope of the $m_{\text{eff}}^{(at)}(Q^2)$, as can be seen from Fig. 3. This is the smallest slope found in all considered channels: $m_{\text{eff}}(Q^2)$ drops from its “constituent” value of about 380 MeV to about 320 MeV at $Q^2 \sim 3 \text{ GeV}^2$ and saturates there. In particular, m_{eff} does not vanish at any finite Q^2 , i.e. there is no indication for chiral restoration in this channel. (In order to obtain a restoration transition, the coupling λ_{at} would have to be about 3 times larger than the phenomenological estimate, i.e. $\lambda_{at} \geq 3\lambda_{a_1}$.) In view of the similarities and the chiral relation with the vector channel, this result might seem surprising. Perhaps it is an indication for the constituent-quark picture to fail at the rather large scales set by the mass of the a_1 (1260). In any case, the qualitative difference between the behavior of m_{eff} in the vector and axial-vector channels supplies our probably least expected case of channel-dependence in the RDQM approach since, in contrast to the pseudoscalar correlator, both vector and axial-vector resonances are well described by the NRQM.
4. The scalar-isovector channel is singled out by the fact that neither in the lattice nor in the instanton-liquid and phenomenological [27] data the pole of the lowest-lying resonance could be resolved. Our qualitative analysis in section III B established that in this case the effective quark mass cannot vanish, so that there exists no finite Q_c^2 in this channel. This is confirmed by the numerical analysis, as shown in Fig. 4. (Unfortunately, lattice data for the scalar-isoscalar point-to-point correlator do not yet exist. This prevents us from studying the isospin-dependence in the scalar channel and in the delineated effective quark masses (cf. section III C) quantitatively.)

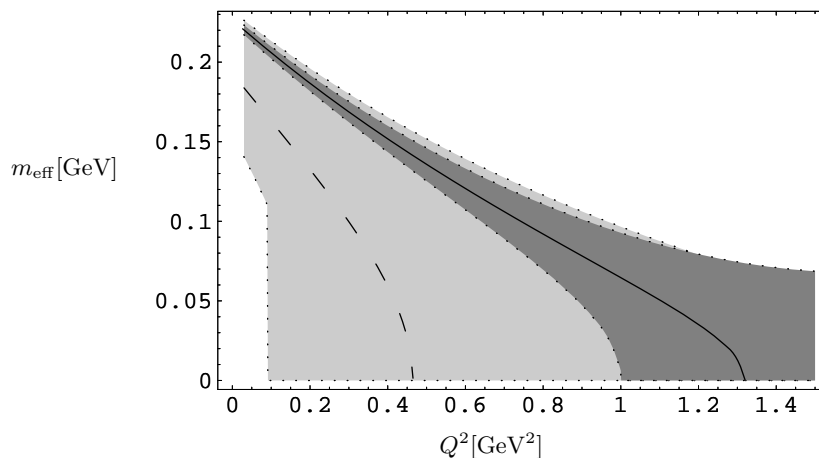


FIG. 2: The resolution-dependent quark mass as obtained from the vector correlator. The input data are taken from the phenomenological estimate of Ref. [6] (solid with dark error band) and the lattice results of Ref. [9] (dashed with light error band). The error bands represent the propagated uncertainties of the input data (cf. Table I).

V. DISCUSSION AND CONCLUSIONS

In our above analysis we have investigated several aspects of resolution-dependent quark masses in hadronic current-current correlation functions. To this end, we have generalized the recently proposed RDQM description [1], based on noninteracting mesonic correlators with a resolution-dependent constituent quark mass $m_{\text{eff}}(Q^2)$, beyond the vector channel. We have then determined the resolution-dependent masses by matching the RDQM correlators to the available experimental and lattice data in the light meson channels. This enables us to clarify several virtues and limitations of the RDQM approach by comparison with a larger body of physical information. While the stringency of such comparative tests is limited by the rather large errors of our input data, it is on the other hand enhanced by the rich variety of physics in the different spin-0 and spin-1 meson channels.

Despite this diversity, we find the small- Q^2 behavior of the effective masses to be relatively channel-independent: in all but the pseudoscalar channel we obtain values in the expected range of about 250 - 350 MeV for $m_{\text{eff}}(0)$. The overall description of mesonic correlators in terms of noninteracting correlators with a unique $m_{\text{eff}}(Q^2)$ and a

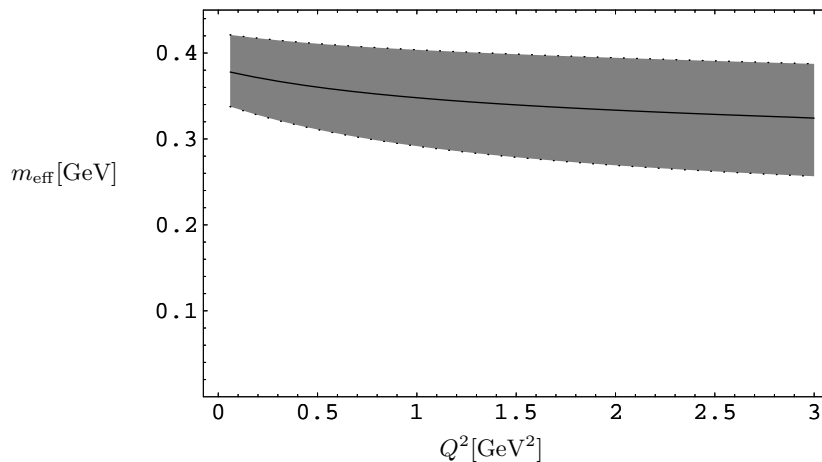


FIG. 3: The resolution-dependent quark mass as obtained from the transverse axial-vector correlator. The input data are taken from the phenomenological estimate of Ref. [6]. Again, the error bands represent the propagated input uncertainties (cf. Table I).

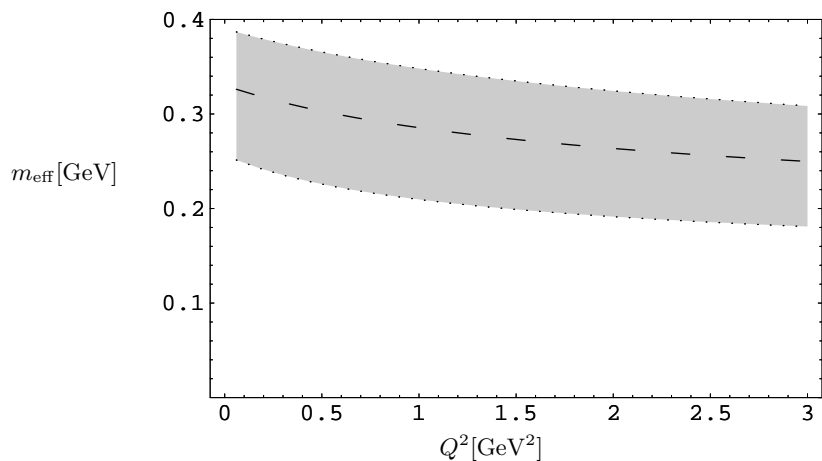


FIG. 4: The resolution-dependent quark mass as obtained from the scalar correlator. The input data are taken from the lattice [9]. Again, the error bands show the propagated input uncertainties (cf. Table I). The resolution-dependent mass cannot vanish in this channel since no resonance is resolved in the input data.

restoration scale $Q_c^2 \sim \Lambda_\chi^2$, however, does not generalize beyond the vector-meson channel. In fact, we do not find an even approximately universal effective mass: first of all, and as expected, the RDQM method cannot reproduce the pseudoscalar correlator with a physically reasonable constituent mass. Secondly, it also fails to generalize to channels like the axial-vector one whose ground-state resonances are quark-model states. This is more surprising since the approach was conceived in a nonrelativistic quark model setting. Furthermore, nonperturbative enhancements of flavor-symmetry breaking, as they manifest themselves e.g. in the substantial differences between the isoscalar and isovector 0^{++} correlators, are not captured. Even the vanishing of m_{eff} at a finite Q_c^2 , related to chiral symmetry restoration and thus expected to be a rather robust feature, is realized only in the vector correlator.

The above shortcomings can be traced to essentially one common root: the various correlator channels differ only in the Dirac and flavor structure of their interpolating fields, and consequently all channel dependence of the RDQM correlators is contained exclusively in the weights of chirally even and odd combinations of the *free* Dirac propagators in the spin and flavor traces. The differences between those weights are of order unity and hence cannot generate the pronounced channel patterns found in the input data for the interacting correlators. If one nevertheless insists on matching free correlators with Q^2 -dependent quark masses to those input data, one is bound to obtain strongly channel-dependent effective masses. Thus the RDQM parametrization is inconsistent with the assumption of the constituent-quark picture that the basic properties of constituent quarks do not depend on the hadron channel in

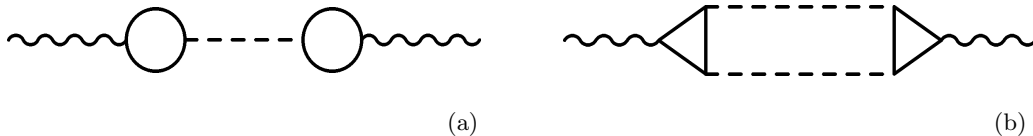


FIG. 5: Two types of corrections to the hadronic correlators within a chiral quark model. The external currents are represented by wavy, quarks by straight and chiral σ and π mesons by dashed lines.

which they are probed. This finding strongly suggests that the minimal RDQM approach, describing all correlators by just a free quark loop with resolution-dependent masses, overburdens those masses with the task of mocking up dynamics which should play itself out elsewhere.

From a microscopic point of view this is not surprising. A consistent RG-treatment of any quark dynamics would generate, besides the explicit interactions, a resolution dependence not only for the quark mass but also for the couplings and interpolating currents. As an illustrative example, consider the qualitative distinction between vector and axial-vector channels which comes about because only the non-conserved axial-vector interpolator gets renormalized. The lack of this effect in the RDQM approach might at least partially explain the absence of a restoration transition in the axial-vector channel.

Since the free quark loop is the leading contribution to the correlators in relativistic chiral quark models, it is suggestive to consult such models in search for a systematic improvement of the minimal RDQM approach. Additional incentive for the use of this framework derives from the fact that a resolution dependence of the quark mass emerges naturally as a cutoff-scale dependence in the RG flow of chiral quark models [3, 4], and that chiral symmetry breaking and restoration arise dynamically.

To low orders in the quark-meson interactions, typical corrections due to the exchange of σ - and π -mesons in such models are shown diagrammatically in Fig. 5. It is tempting to speculate about their qualitative impact and about whether the absence of such contributions in the minimal RDQM approach might explain some of its shortcomings. The pole diagram (a) contributes only in the pseudoscalar and longitudinal axial-vector channels [28] where a pion is exchanged. Since this contribution is very strongly attractive, it is likely that its neglect prevents a minimal RDQM description of the corresponding correlators with a constituent mass of the typical size. Diagram (b) contributes in the scalar, pseudoscalar, vector and axial-vector channels through vertices with the meson content $\vec{\pi} \times \vec{\pi}$, $\sigma\vec{\pi}$, $\vec{\pi} \times \partial_\mu \vec{\pi}$ and $\sigma\partial_\mu \vec{\pi}$, respectively. The contribution to the vector correlator is therefore mediated solely by Goldstone bosons. Hence the ensuing corrections set in at very low Q^2 . In the minimal RDQM correlator, on the other hand, the absence of the corresponding strength can only be compensated by a smaller constituent quark mass $m_{\text{eff}}^{(v)}(Q^2 \sim 0)$. This might explain why we indeed find $m_{\text{eff}}^{(v)}(0)$ to be somewhat lower than the typical constituent mass scale. The lighter constituent mass might also facilitate the restoration transition in the vector relative to the transverse axial-vector channel.

In contrast, the corrections of type (b) to the axial-vector channel set in at higher Q^2 since the more massive σ -meson participates. These contributions should be negligible at small Q^2 , rendering $m_{\text{eff}}^{(at)}(0)$ our perhaps most reliable estimate for the constituent mass. Moreover, since corrections of type (b) with a σ - π pair exchanged can contribute strongly at momenta $Q^2 \sim \Lambda_\chi^2$ close to the typical restoration scale, their neglect may be partially responsible for the absence of a chiral-restoration transition in the transverse axial-vector RDQM correlator. In the scalar channel the situation is less conclusive. Since a pion pair can be exchanged in this channel, too, it is not a priori clear why we obtain a reasonable constituent mass value for $m_{\text{eff}}^{(s)}(0)$ although this correction is neglected in the RDQM approach.

The above qualitative arguments, although tentative, give some hints as to why the minimal RDQM treatment does not generalize, with an approximately universal $m_{\text{eff}}(Q^2)$, beyond the vector channel. It remains an interesting and open question to which extent a more sophisticated dynamical treatment, e.g. in the context of chiral quark models, could achieve a unified description of the variety among hadron correlators on the basis of universal, resolution-dependent quark masses.

VI. APPENDIX

In this appendix, we analyze the two equations (25, 26) in detail and derive conditions for the existence, general properties and channel dependence of the critical scale Q_c^2 defined in section III B. Since the involved hadronic scales are mutually too close to allow for useful approximations and since the exact solutions are less than transparent, we

resort to an indirect approach.

For the spin-0 channels, we start by rearranging Eq. (25) into

$$L_{s/p} \left(Q_c^2; m_{s/p}^2, s_0 \right) \equiv \frac{s_0^2 \left(m_{s/p}^2 + Q_c^2 \right)^3}{Q_c^2 (s_0 + Q_c^2)^2} = \frac{16\pi^2}{N_c} \lambda_{s/p}^2, \quad (29)$$

whose left-hand side has the derivative

$$\frac{\partial L_{s/p} \left(Q_c^2; m_{s/p}^2, s_0 \right)}{\partial Q_c^2} = - \frac{s_0^2 \left(m_{s/p}^2 + Q_c^2 \right)^2 \left[m_{s/p}^2 (3Q_c^2 + s_0) - 2Q_c^2 s_0 \right]}{Q_c^4 (s_0 + Q_c^2)^3}. \quad (30)$$

1. For $s_0 < 3m_{s/p}^2/2$ we read off [29] from (30) that $L_{s/p}$ decreases monotonically with Q_c^2 towards its limiting value s_0^2 at $Q_c^2 \rightarrow \infty$. Thus there is no solution if $L_{s/p}(Q^2)$ does not cross the horizontal line corresponding to the right-hand side of (29), i.e. if $16\pi^2 \lambda_{s/p}^2 / N_c < s_0^2$. Hence one (finite) solution exists for $s_0^2 < 16\pi \lambda_{s/p}^2 / N_c$, otherwise there is none.
2. For $s_0 > 3m_{s/p}^2/2$, which holds for our input data (in the pseudoscalar channel), $L_{s/p}(Q^2)$ is monotonically decreasing in the range $0 < Q_c^2 < s_0 m_{s/p}^2 / (2s_0 - 3m_{s/p}^2)$ towards its minimum

$$L_{s/p}^{(\min)} \left(m_{s/p}^2, s_0 \right) \equiv \frac{27}{4} \frac{m_{s/p}^4}{s_0} \left(s_0 - m_{s/p}^2 \right) \quad (31)$$

and monotonically increasing for $Q_c^2 > s_0 m_{s/p}^2 / (2s_0 - 3m_{s/p}^2)$ towards its limiting value s_0^2 at $Q_c^2 \rightarrow \infty$. As a consequence, there are three cases to distinguish for the solutions of Eq. (25), corresponding to the number of intersections between $L_{s/p}(Q_c^2)$ and the right-hand side of (29):

(a) no solution for

$$L_{s/p}^{(\min)} \left(m_{s/p}^2, s_0 \right) > \frac{16\pi^2}{N_c} \lambda_{s/p}^2, \quad (32)$$

(b) one solution for

$$L_{s/p}^{(\min)} \left(m_{s/p}^2, s_0 \right) = \frac{16\pi^2}{N_c} \lambda_{s/p}^2 \quad \text{and for} \quad s_0^2 < \frac{16\pi^2}{N_c} \lambda_{s/p}^2, \quad (33)$$

(c) two solutions for

$$L_{s/p}^{(\min)} \left(m_{s/p}^2, s_0 \right) < \frac{16\pi^2}{N_c} \lambda_{s/p}^2 \leq s_0^2. \quad (34)$$

The above analysis implies that there is a bound on the smallest, i.e. physical solution (if there are two) given by the Q_c^2 where $L_{s/p}$ has its minimum,

$$Q_c^2 < \frac{s_0 m_{s/p}^2}{2s_0 - 3m_{s/p}^2}. \quad (35)$$

A somewhat stronger bound, namely the finite and positive solution of $L_{s/p}(Q_c^2; m_{s/p}^2, s_0) = s_0^2$, applies in the case of one unique solution.

The analogous analysis for the spin-1 channels is slightly more involved. We start from Eq. (26) in the form

$$L_{v/at} \left(Q_c^2; m_{v/at}^2, s_0 \right) \equiv \frac{s_0 (s_0 + 2Q_c^2) \left(m_{v/at}^2 + Q_c^2 \right)^3}{Q_c^4 (s_0 + Q_c^2)^2} = \frac{24\pi^2}{N_c} \lambda_{v/at}^2. \quad (36)$$

Its derivative

$$\frac{\partial L_{v/at} (Q_c^2; m_{v/at}^2, s_0)}{\partial Q_c^2} = - \frac{s_0 (m_{v/at}^2 + Q_c^2)^2 [2m_{v/at}^2 (3Q_c^4 + 3Q_c^2 s_0 + s_0^2) - Q_c^2 s_0 (3Q_c^2 + s_0)]}{Q_c^6 (s_0 + Q_c^2)^3} \quad (37)$$

is (for $Q_c^2, s_0 > 0$) positive/negative if

$$3 (2m_{v/at}^2 - s_0) Q_c^4 + s_0 (6m_{v/at}^2 - s_0) Q_c^2 + 2s_0^2 m_{v/at}^2 \leq 0. \quad (38)$$

The associated quadratic equation has the solutions

$$\tilde{Q}_{c1,2}^2 = \frac{s_0}{6 (2m_{v/at}^2 - s_0)} \left[s_0 - 6m_{v/at}^2 \pm \sqrt{(s_0 + 6m_{v/at}^2)^2 - 48m_{v/at}^4} \right] \quad (39)$$

(where \tilde{Q}_{c1}^2 (\tilde{Q}_{c2}^2) corresponds to the + (-) sign in front of the square root) which determine the boundaries of the monotonicity intervals of $L_{v/at} (Q_c^2)$. As above, the duality parametrization of the spectral functions requires $s_0 > m^2$ so that the square root in Eq. (39) is real and larger than $m_{v/at}^2$. To proceed further, we have again to distinguish between two alternative, more restrictive conditions on s_0 :

1. For $m_{v/at}^2 < s_0 < 2m_{v/at}^2$, which is satisfied by part of our input data in the vector channel and all of those

in the axial-vector channel, we have $m_{v/at}^2 < \sqrt{(s_0 + 6m_{v/at}^2)^2 - 48m_{v/at}^4} < 4m_{v/at}^2$, and positive solutions \tilde{Q}_c^2 require the square bracket in Eq. (39) to be positive. This is easily seen to be impossible (for \tilde{Q}_{c1}^2 it takes values in $[-4, 0] \times m_{v/at}^2$ and for \tilde{Q}_{c2}^2 in $[-8, -6] \times m_{v/at}^2$). Thus both solutions of Eq. (39) are negative and $L_{v/at} (Q_c^2)$ is monotonically decreasing for all $Q^2 > 0$, down to its limiting value $2s_0$ at $Q^2 \rightarrow \infty$. As a consequence, we have one (finite) solution for

$$\frac{24\pi^2}{N_c} \lambda_{v/at}^2 > 2s_0 \quad (40)$$

and none otherwise.

2. For $s_0 > 2m_{v/at}^2$, which is satisfied by part of our input data in the vector channel and implies

$\sqrt{(s_0 + 6m_{v/at}^2)^2 - 48m_{v/at}^4} > 4m_{v/at}^2$, positive solutions \tilde{Q}_c^2 require the square bracket in Eq. (39) to be negative. For the solution \tilde{Q}_{c1}^2 this is impossible while it generally holds for \tilde{Q}_{c2}^2 . The desired solution is thus \tilde{Q}_{c2}^2 , and $L_{v/at} (Q_c^2)$ is monotonically decreasing for $0 < Q_c^2 < \tilde{Q}_{c2}^2$ down to its minimum

$$L_{v/at}^{(\min)} (m_{v/at}^2, s_0) \equiv \frac{(s_0^2 + 12m_{v/at}^2 s_0 - 12m_{v/at}^4)^{3/2} - s_0 (s_0^2 - 36m_{v/at}^2 s_0 + 36m_{v/at}^4)}{8s_0^2} \quad (41)$$

at \tilde{Q}_{c2}^2 , and monotonically increasing for $Q_c^2 > \tilde{Q}_{c2}^2$ up to its limiting value $2s_0$ for $Q_c^2 \rightarrow \infty$. Again, the solutions of Eq. (36) are obtained by the intersections of $L_{v/at} (Q_c^2)$ with its right-hand side, and we find three cases:

- (a) no solution for

$$L_{v/at}^{(\min)} (m_{v/at}^2, s_0) > \frac{24\pi^2}{N_c} \lambda_{v/at}^2, \quad (42)$$

- (b) one solution for

$$L_{v/at}^{(\min)} (m_{v/at}^2, s_0) = \frac{24\pi^2}{N_c} \lambda_{v/at}^2 \quad \text{and for} \quad 2s_0 < \frac{24\pi^2}{N_c} \lambda_{v/at}^2, \quad (43)$$

- (c) two solutions for

$$L_{v/at}^{(\min)} (m_{v/at}^2, s_0) < \frac{24\pi^2}{N_c} \lambda_{v/at}^2 \leq 2s_0. \quad (44)$$

Again, there is a bound on the physical Q_c^2 (i.e. the smaller one if there are two), namely $Q_c^2 < \tilde{Q}_{c2}^2$, which can be sharpened in case of a unique Q_c^2 where it becomes the positive and finite solution of $L_{v/at}(Q_c^2; m_{v/at}^2, s_0) = 2s_0$.

To summarize: a ‘‘chiral restoration’’ transition to a vanishing quark mass with a unique solution Q_c^2 (for $s_0 > m_{v/at}^2$) requires

$$s_{0,s/p}^2 < \frac{16\pi^2}{N_c} \lambda_{s/p}^2, \quad s_{0,v/at} < \frac{12\pi^2}{N_c} \lambda_{v/at}^2 \quad (45)$$

(note that these conditions are independent of the resonance mass) while under the more restrictive conditions $s_{0,s/p} > 3m_{s/p}^2/2$ and $s_{0,v/at} > 2m_{v/at}^2$ (which are satisfied by several of our input parameter sets) also two solutions are possible (with the lower one being physical) if

$$L_{s/p}^{(\min)}(m_{s/p}^2, s_0) < \frac{16\pi^2}{N_c} \lambda_{s/p}^2 \leq s_0^2, \quad L_{v/at}^{(\min)}(m_{v/at}^2, s_0) < \frac{24\pi^2}{N_c} \lambda_{v/at}^2 \leq 2s_0. \quad (46)$$

Given any input data set for a correlator with the corresponding values for m , λ and s_0 , the above results instantly reveal whether the extracted m_{eff} will vanish at some finite Q_c .

With the data in Table I (taking the central values) we predict a vanishing effective quark mass in the pseudoscalar channel (with a unique solution for Q_c) as well as in the vector channel for the phenomenological, lattice I and II (with the lower of two solutions for Q_c), but not for the ILM data, and no ‘‘chiral restoration’’ in the axial-vector channel (the ILM data in this channel are excluded since they do not satisfy $m_{at}^2 < s_0$).

Acknowledgments

We would like to thank Hans-Jürgen Pirner for interesting discussions. This work was partially supported by the Kovalevskaja Program of the Alexander-von-Humboldt Foundation, the German Research Council (DFG), and the German Ministry for Education and Research (BMBF).

-
- [1] H. G. Dosch, T. Gousset and H. J. Pirner, Phys. Rev. D **57**(1998) 1666 [arXiv:hep-ph/9707264].
 - [2] K. G. Wilson and J. B. Kogut, Phys. Rept. **12**(1974) 75.
 - [3] J. Meyer, K. Schwenzer, H. J. Pirner and A. Deandrea, Phys. Lett. B **526**(2002) 79 [arXiv:hep-ph/0110279]; B. J. Schaefer and H. J. Pirner, Nucl. Phys. A **660** (1999) 439 [arXiv:nucl-th/9903003].
 - [4] J. Berges, D. U. Jungnickel and C. Wetterich, Phys. Rev. D **59**(1999) 034010 [arXiv:hep-ph/9705474].
 - [5] V.A. Novikov, M.A. Shifman, A.I. Vainshtein, and V.I. Zakharov, Nucl. Phys. B **191** (1981) 301.
 - [6] E. V. Shuryak, Rev. Mod. Phys. **65**(1993) 1.
 - [7] M. Shifman, hep-ph/0009131, in M. Shifman (ed.): *At the frontier of particle physics, Handbook of QCD*, vol. 3, p. 1447-1494 (World Scientific, Singapore, 2001).
 - [8] M.A. Shifman, A.I. Vainshtein, and V.I. Zakharov, Nucl. Phys. B **147** (1979) 385.
 - [9] M. C. Chu, J. M. Grandy, S. Huang and J. W. Negele, Phys. Rev. D **48**(1993) 3340 [arXiv:hep-lat/9306002].
 - [10] S. J. Hands, P. W. Stephenson and A. McKerrell [UKQCD Collaboration], Phys. Rev. D **51**(1995) 6394 [arXiv:hep-lat/9412065].
 - [11] M. C. Chu, J. M. Grandy, S. Huang and J. W. Negele, Phys. Rev. D **49**(1994) 6039 [arXiv:hep-lat/9312071].
 - [12] T. DeGrand, Phys. Rev. D **64** (2001) 094508 [arXiv:hep-lat/0106001].
 - [13] J. Negele, private communication.
 - [14] E. V. Shuryak and J. J. Verbaarschot, Nucl. Phys. B **410**(1993) 55 [arXiv:hep-ph/9302239].
 - [15] D. E. Groom *et al.*[Particle Data Group Collaboration], Eur. Phys. J. C **15**(2000) 1.
 - [16] S. Coleman, *Aspects of Symmetry*, Cambridge University Press 1988.
 - [17] The RDQM approach is restricted to the spacelike momentum region of the correlators.
 - [18] As in [1], however, one should expect some n -dependence in the resulting $m_{\text{eff}}(Q^2)$.
 - [19] The resulting $m(Q^2)$ of Ref. [1] is to good accuracy (5%) given by the linear parametrization $m(Q^2) \simeq (0.22 \text{ GeV}) (1 - Q^2/Q_c^2)$ with $Q_c^2 = 1.05 \text{ GeV}^2$.
 - [20] Initially, we had included the cooled lattice data of Ref. [11] in our analysis, in the hope to delineate information about the role of instantons in generating the hadronic input parameters. It turned out, however, that the RDQM method cannot resolve significant differences between the cooled and uncooled data.
 - [21] We do not use the recent lattice data [12] from overlap fermions since those are restricted to relatively short distances, lack small-mass extrapolation and might be subject to rather large finite-size corrections [13].

- [22] For transparency of notation we have suppressed the channel labels of $s_{0,i}$ and $Q_{c,i}$.
- [23] A somewhat stronger bound, given in the appendix, can be established in the case of a unique solution.
- [24] Note that isospin-violating disconnected contributions could provide an exception to this rule in channels which carry vacuum quantum numbers.
- [25] In the vector channel, the differences between isoscalar and isovector correlators are less pronounced.
- [26] Note that the resolution-dependent mass extracted from the ILM data does not vanish at any Q^2 . This might be related to the significantly larger constituent mass $m_{\text{eff}}^{(v)}(0)$ obtained in the ILM (cf. Table I). Similarly large constituent masses together with the absence of a chiral restoration transition are also found in the axial-vector channel (see below).
- [27] The $a_0(980)$ resonance is commonly interpreted as a 4-quark state and therefore not included in the phenomenological analysis of Ref. [6].
- [28] Recall that we only consider isovector interpolators.
- [29] More precisely, s_0 lies in the interval $m_{s/p}^2 < s_0 < 3m_{s/p}^2/2$ since the resonance-continuum parametrization (14) additionally requires $s_0 > m_{s/p}^2$.